

Unambiguous measurement of information scrambling in a hierarchical star-topology system

Deepak Khurana,^{*} V. R. Krithika,[†] and T. S. Mahesh[‡]

*Department of Physics and NMR Research Center,
Indian Institute of Science Education and Research, Pune 411008, India*

We investigate the scrambling of information in a hierarchical star-topology system using out-of-time-ordered correlation (OTOC) functions. The system consists of a central qubit directly interacting with a set of satellite qubits, which in turn interact with a second layer of satellite qubits. This particular topology not only allows convenient preparation and filtering of multiple quantum coherences between the central qubit and the first layer but also engineer scrambling in a controlled manner. Hence, it provides us with an opportunity to experimentally study scrambling of information localized in multi-spin correlations via the construction of relevant OTOCs. Since the measurement of OTOC requires a time evolution, the non-scrambling processes such as decoherence and certain experimental errors create an ambiguity. Therefore, the unambiguous quantification of information scrambling requires suppressing contributions from decoherence to the OTOC dynamics. To this end, we propose and experimentally demonstrate a constant time protocol which is able to filter contribution exclusively from information scrambling.

PACS numbers: 03.65.Yz, 03.67.a

Keywords: Multiple quantum coherences, Information scrambling, Out-of-time ordered correlation functions

I. INTRODUCTION

Scrambling of initially localized quantum information into many degrees of freedom via the creation of non-local correlations leads to a perceived loss of quantum information in practical time scales. In recent investigations, measurement of information scrambling has been related to many practical aspects such as diagnosis of quantum chaos [1–3], entanglement [4], detection of many-body localization [5–8], quantum phase transitions [9, 10], and thermalization [11]. The center to all these studies is the experimentally measurable physical quantity called the out-of-time-ordered correlation (OTOC) functions [1, 2, 12]. An OTOC function is four point correlation function where the operators are not ordered in time, and its temporal decay is taken as indication of information scrambling in a many-body quantum system [13]. Despite significant theoretical investigations across condensed matter and high-energy research, experimental measurement of OTOC functions is challenging because it involves the reversal of time evolution. Several protocols such as interferometric [14, 15], quantum clock [16], and quasi-probabilities [17] are proposed. On the experimental side, early success with nuclear magnetic resonance (NMR) [5, 18, 19] and ion-traps platforms [20, 21] have been reported.

In realistic scenarios, decoherence and experimental errors also contribute to the decay of OTOC, and thereby create an ambiguity in the observation of information scrambling [21, 22]. To address this issue, methods based

on the use of quantum teleportation [20, 23] and OTOC quasi-probabilities [24] have been put forward recently for verified measurement of information scrambling.

Till now, experimental studies have largely focused on the investigation of scrambling of information localized in uncorrelated degrees of freedom. Recently, the scrambling of information localized in many-body correlations, such as multiple quantum coherences (MQCs) has also been reported [19]. MQCs have been used for practical purposes such as quantum sensing [25], detecting entanglement [4], noise spectroscopy [26] to name a few which makes it imperative to study the impact of scrambling on these states.

In this regard, star-topology systems are well suited for this purpose because they allow a controlled and convenient preparation of various MQCs [25, 27]. Further, if the star-topology system has multiple layers, it provides an opportunity to study scrambling of information localized in multi-spin correlations of inner layers to outer layers. Such hierarchical star-topology systems (HSTS) are important not only from the perspective of studying information scrambling but also they can be treated as a model for realistic environments to study dynamics of open quantum systems. For example, ¹⁵N impurities around a nitrogen vacancy center in diamond acts the first layer and surrounding ¹³C spins constitute the second layer [28].

In this work, using nuclear magnetic resonance (NMR) methods, we study information scrambling in a HSTS consisting of a central qubit surrounded by two layers of satellite qubits. We can initialize the system in a desired MQC between the central qubit and the first layer. Subsequently, we drive the dynamics from the scrambling to non-scrambling regime by tuning the nonintegrability of evolution propagator. Moreover, we propose a constant time protocol (CTP) to solely capture the scrambling

^{*}Electronic address: deepak.khurana@students.iiserpune.ac.in

[†]Electronic address: krithika_vr@students.iiserpune.ac.in

[‡]Electronic address: mahesh.ts@iiserpune.ac.in

dynamics while disregarding the decoherence effects. Finally, we experimentally demonstrate the CTP protocol for the exclusive study of scrambling dynamics of a specific MQC.

The paper is organized as follows: In the following section, we briefly review the OTOC formalism and introduce CTP. In section III, we describe the experimental system and explain MQC preparation. In section IV, we first investigate the OTOC dynamics corresponding to various MQCs by numerical methods. Further, we describe the experimental study of the scrambling dynamics of a particular MQC using CTP. Finally, we conclude in section V.

II. OTOC FUNCTION AND ITS UNAMBIGUOUS MEASUREMENT

Consider two operators $B(t)$ and $A(0)$, with commutator $C(t) = [A(0), B(t)]$ and let $C(0) = 0$. OTOC function is then defined as [1, 2, 12]

$$\mathcal{O}(t) = \langle B^\dagger(t)A^\dagger(0)B(t)A(0) \rangle_\beta, \quad (1)$$

where $B(t) = U^\dagger(t)B(0)U(t)$ is evolved in Heisenberg picture with unitary operator $U(t) = e^{-i\mathcal{H}t}$ with $\hbar = 1$. Here \mathcal{H} is the Hamiltonian governing the system dynamics and $\langle * \rangle_\beta = \text{Tr}(* \cdot e^{-\beta\mathcal{H}})/Z$ is the average over a thermal ensemble prepared with a temperature $1/(k_B\beta)$, with k_B being the Boltzmann constant and $Z = \text{Tr}(e^{-\beta\mathcal{H}})$ being the partition function. If $A(0)$ and $B(t)$ are unitaries, then the OTOC function can be related to the norm of the commutator $C(t)$ by

$$\mathcal{O}(t) = \text{Re}[\mathcal{O}(t)] = 1 - \frac{1}{2} \langle C^\dagger(t)C(t) \rangle_\beta. \quad (2)$$

In general, as $\mathcal{O}(t)$ evolves under the unitary $U(t)$, it exhibits occasional revivals to unity unless there exists a loss of information. This loss of information is either due to decoherence or due to the leakage of information via scrambling. In either case, the above commutation norm fails to vanish over time, thus preventing the OTOC revivals. However, in practice, both of these effects lead to an effective loss of OTOC revivals in practical timescales.

In the following we assume $A(0) = \rho(0)$, the initial state of the system and $B(t)$ is a unitary operator. Let us consider following two extreme cases.

(i) A pure initial state ($\rho^2(0) = \rho(0)$) corresponding to zero temperature, i.e., $\beta \rightarrow \infty$. In this case

$$\begin{aligned} \mathcal{O}(t) &= \text{Re}[\langle B^\dagger(t)\rho^\dagger(0)B(t)\rho(0) \rangle_{\beta \rightarrow \infty}] \\ &= \text{Re}[\text{Tr}\{B^\dagger(t)\rho(0)B(t)\rho(0)\}]. \end{aligned} \quad (3)$$

(ii) A highly mixed qubit state corresponding to high-temperature NMR conditions, $\rho(0) = \mathbb{1}/2 + \epsilon\rho_\Delta(0)$, where the traceless part $\rho_\Delta(0)$ is often termed as the deviation density matrix. Here $\epsilon \propto \beta \simeq 0$ is the purity

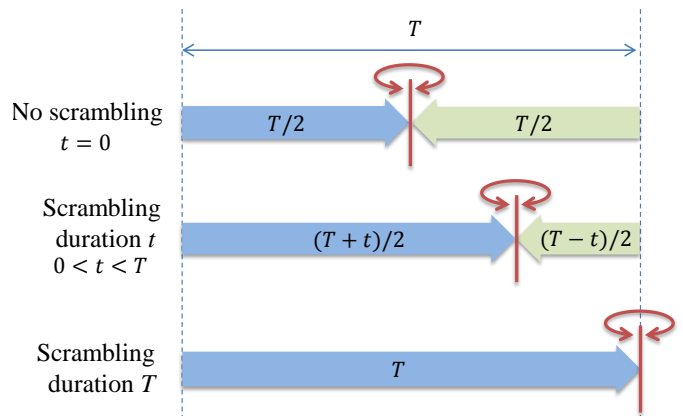


FIG. 1: Schematic illustration of CTP protocol. The blue and green bars indicate forward and backward evolutions respectively. While decoherence is active throughout the duration T , scrambling is active only for the net forward evolution time t .

factor. Now,

$$\begin{aligned} \mathcal{O}(t) &= \text{Re}[\langle B^\dagger(t)\rho^\dagger(0)B(t)\rho(0) \rangle_{\beta \rightarrow 0}] \\ &\sim \text{Re}[\text{Tr}\{B^\dagger(t)\rho_\Delta(0)B(t)\rho_\Delta(0)\}], \end{aligned} \quad (4)$$

up to ϵ^2 factor and a constant background (see Appendix A).

Moreover, if $B^\dagger(t) = U(t)$ is the evolution propagator, then

$$\mathcal{O}(t) = \langle \rho(t) | \rho(0) \rangle \quad \text{or} \quad \langle \rho_\Delta(t) | \rho_\Delta(0) \rangle \quad (5)$$

as is relevant. Thus in this setting, $\mathcal{O}(t)$ can be measured by the overlap between the instantaneous state with the initial state.

In order to perform an exclusive study of scrambling, it is important to separate the decoherence effects. To this end, certain protocols based on OTOC quasi probabilities [17, 24] and quantum teleportation [20, 23] have been proposed. In the following we propose an alternate approach based on the constant-time protocol (CTP) (illustrated in Fig.1) commonly used in multi-dimensional NMR spectroscopy [29].

We decompose the time-evolution unitary $U(t)$ into two parts,

$$\begin{aligned} U(t) &= e^{-i\mathcal{H}t} \\ &= e^{i\mathcal{H}(T-t)/2} e^{-i\mathcal{H}(T+t)/2} \\ &= U^\dagger\left(\frac{T-t}{2}\right) U\left(\frac{T+t}{2}\right). \end{aligned} \quad (6)$$

Thus scrambling under the unitary effectively happens only for time t , but the decoherence is active throughout the total time T . Hence by carrying out multiple experiments by varying t for an experimentally feasible fixed T , one can reconstruct unambiguous evolution under scram-

bling Hamiltonian. This protocol can be incorporated in all the standard OTOC measurement methods [4, 14–19, 21].

III. COMBINATION MQCS IN A HSTS

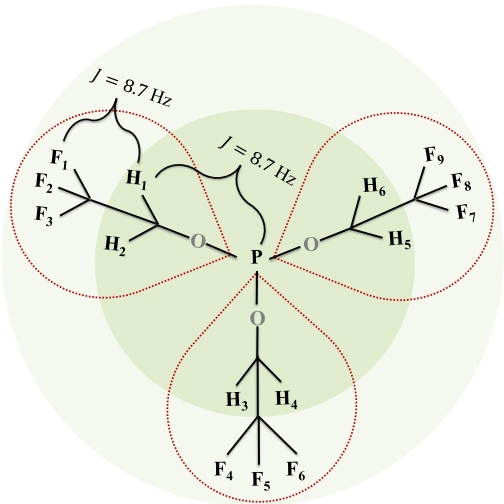


FIG. 2: Molecule structure of tris(2,2,2-trifluoroethyl) phosphite. One ^{31}P spin, six ^1H spins and nine ^{19}F spins act as central spin, first and second layer respectively. Each branch constitutes one ^{31}P spin, two ^1H spins and three ^{19}F spins.

In this work, we consider an N -qubit HSTS with a central qubit surrounded by N_1 qubits in the first layer and N_2 qubits in the second layer. Specifically, the experimental NMR system consists of a ^{31}P spin surrounded by a layer of six equivalent ^1H spins. Each of ^1H spin is further coupled to three ^{19}F spins in the second layer, as shown in Fig 2. Such a system allows us to explore controlled scrambling of information stored in correlations of the central qubit with the first layer to the second layer.

Let $\hbar = 1$, $\alpha \in \{x, y, z\}$, and σ_α^P , $\sigma_{i\alpha}^H$ and $\sigma_{j\alpha}^F$ be Pauli- α operators for ^{31}P , i th ^1H and j th ^{19}F respectively. We also define the collective terms

$$H_\alpha = \sum_{i=1}^{N_1} \sigma_{i\alpha}^H \quad \text{and} \quad F_\alpha = \sum_{j=1}^{N_2} \sigma_{j\alpha}^F.$$

The Hamiltonian of a K -branch system can be written as a sum of internal interactions and external fields,

$$\mathcal{H}_K = \sum_{k=1}^K \mathcal{H}_{\text{int}}^{(k)} + \mathcal{H}_{\text{ext}}^{(k)}. \quad (7)$$

The branch-wise decomposition of the Hamiltonian is convenient for numerical simulations of OTOC dynamics with partial system size. Here the k th branch internal

interaction Hamiltonian is

$$\mathcal{H}_{\text{int}}^{(k)} = \frac{\pi J}{2} \left(\sum_{i=1}^2 \sigma_z^P \sigma_{mz}^H + \sum_{i=1}^2 \sum_{j=1}^3 \sigma_{mz}^H \sigma_{nz}^F \right), \quad (8)$$

where $m = 2(k-1) + i$ and $n = 3(k-1) + j$. Thus, in each branch, the central ^{31}P spin is coupled to two ^1H spins and each ^1H spin is further coupled to three ^{19}F spins. In our system, $J = 8.7$ Hz happens to be the single scalar coupling constant.

The external Hamiltonian $\mathcal{H}_{\text{ext}}^{(k)}$ on the k th branch constitutes the application of equal amplitudes gJ of x and z fields employed to introduce non-integrability in the dynamics:

$$\mathcal{H}_{\text{ext}}^{(k)} = \frac{gJ\pi}{2} \sum_{\alpha \in x, z} \left(\sigma_\alpha^P + \sum_{i=1}^2 \sigma_{m\alpha}^H + \sum_{j=1}^3 \sigma_{n\alpha}^F \right). \quad (9)$$

The impact of system size and decoherence for such as HSTS are discussed in Appendix B.

Now we describe the preparation of combination MQCs between the central qubit and the first layer. Suppose the central spin ^{31}P is initialized in $|\pm\rangle^P = (|0\rangle^P \pm |1\rangle^P)/\sqrt{2}$ and the surrounding ^1H spins are in the state

$$|\xi_n^{N_1}\rangle = |N_1 - n, n\rangle^H \quad (10)$$

indicating $N_1 - n$ spins in $|0\rangle$ state and $n \in [0, N_1]$ spins in $|1\rangle$ state. We now apply a CNOT gate

$$U_c = \{(|0\rangle\langle 0|^P \otimes \mathbb{1}^H + (|1\rangle\langle 1|^P \otimes H_x)\} \otimes \mathbb{1}^F = U_c^\dagger \quad (11)$$

with central ^{31}P spin as the control and surrounding ^1H spins as target. The resulting state is

$$\rho_q^\pm(0) = |\psi_q^\pm\rangle\langle\psi_q^\pm| \otimes \mathbb{1}^F / 2^{N_2} \quad (12)$$

with

$$|\psi_q^\pm\rangle = \frac{|0\rangle^P |\xi_n^{N_1}\rangle \pm |1\rangle^P |\xi_{N_1-n}^{N_1}\rangle}{\sqrt{2}}, \quad (13)$$

which represents a combination MQC with quantum number

$$q = N_1 - 2n + 1. \quad (14)$$

In the following section, we describe scrambling of information out of these MQCs.

IV. SCRAMBLING DYNAMICS OF COMBINATION MQCS

Following the discussion preceding Eq. 4, we choose

$$\rho_\Delta(0) = \rho_q^x(0) = \rho_q^+(0) - \rho_q^-(0). \quad (15)$$

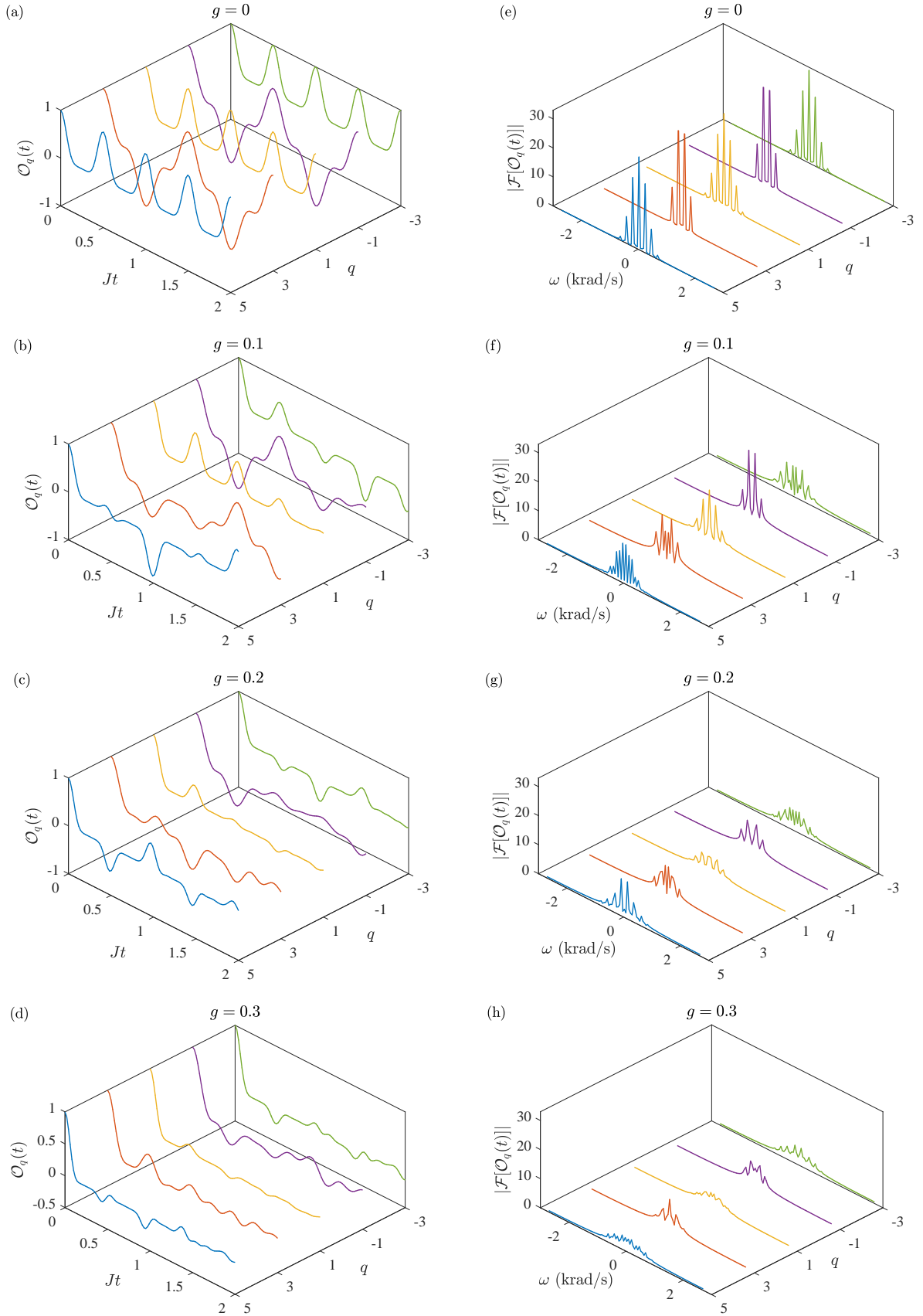


FIG. 3: Simulated time evolutions of OTOC functions for combination MQCs of coherence orders $q \in \{-3, -1, 1, 3, 5\}$ for (a) $g = 0$, (b) $g = 0.1$, (c) $g = 0.2$, and (d) $g = 0.3$. Corresponding Fourier transforms $\mathcal{F}[\mathcal{O}(t)]$ are shown in (e-h). All the simulations are carried out for a two-branch HSTS ($K = 2$). Here no additional decoherence is introduced and all the decays are purely due to the information scrambling.

Therefore, we consider the unambiguous study of OTOC dynamics with the following operators:

$$\begin{aligned} A(0) &= \rho_q^x(0) \quad \text{and} \\ B(t) &= U^\dagger(t). \end{aligned} \quad (16)$$

In this case, the OTOC function becomes

$$\begin{aligned} \mathcal{O}_q(t) &\approx \text{Re} [\langle B^\dagger(t) A^\dagger(0) B(t) A(0) \rangle_{\beta=0}] \\ &= \text{Tr} \{ U(t) \rho_q^x(0) U^\dagger(t) \rho_q^x(0) \} \\ &= \text{Tr} \{ \rho(t) \rho_q^x(0) \}. \end{aligned} \quad (17)$$

The propagator $U(t)$ involves all the spins including those in the second layer and may lead to an effective leakage of coherence from the initial q -quantum combination MQC subspace.

A. Numerical simulations

We have performed the following numerical simulations to gain more insight into the scrambling dynamics of combination MQCs. Considering the computational cost, we simulated only the partial system with $K = 2$ in the Hamiltonian given in Eq. 7. Here no decoherence is introduced, and the observed effects are only due to the scrambling dynamics.

Fig. 3 displays the simulated OTOC for various coherence orders q and Jt for various g values. For the case $g = 0$, the dynamics is integrable, as shown in Fig. 3(a). In this case, the OTOC function shows periodic oscillations for all the MQCs, without any effective decay, suggesting no information scrambling. Note that the profiles of $q = 5$ and $q = -3$ match exactly. This is because, the corresponding states $|\psi_5\rangle$ and $|\psi_{-3}\rangle$ differ only by the state of the central qubit which does not evolve under the scrambling Hamiltonian in the absence of the external fields. Similarly, $q = 3$ and $q = -1$ also match for the same reason.

However, once the external fields are applied, i.e., $g > 0$, the dynamics becomes non-integrable. In this case, the OTOC oscillations become nonperiodic, as shown in Figs. 3(b-d). More importantly, the OTOC profiles now suffer from effective decays due to a gradual loss of information out of the MQC $\rho_q^x(0)$. In fact, the stronger the strength g of the external fields, the more efficient is the scrambling. This dependence of scrambling with nonintegrability of dynamics has also been noted earlier [18] in the context of a spin chain.

Further insight can be obtained by looking at the frequency profiles of OTOC functions. Fig. 3(e-h) display Fourier transforms $\mathcal{F}(\mathcal{O}_q(t))$ for various combination MQCs at different g values. At $g = 0$, the spectral lines are sharp, indicating finite frequency components. However, as we introduce the external fields, i.e., for $g > 0$, we find the emergence of more frequency components, which indicates a stronger leakage of information leading

to more efficient scrambling. As g increases further, we observe an effective smoothing of frequency profiles. At this point, the time domain decay profiles appear almost exponential decays, and therefore, it becomes hard to differentiate them from decoherence induced decays. This fact emphasizes the importance of CTP in practical situations. In the next subsection, we experimentally apply CTP to reveal information scrambling for filtered combination quantum coherence $q = -1$.

B. Experiments

The NMR experiments were carried out in a Bruker NMR spectrometer with a static field of 11.2 T. As described in section III, the sample consisted of tris(2,2,2-trifluoroethyl) phosphite (see Fig. 2) dissolved in deuterated dimethyl sulphoxide (0.05 ml in 0.5 ml). The sample was maintained at an ambient temperature of 298 K. The ^{31}P NMR spectra corresponding various filtered MQCs along with a reference spectrum are shown in Fig. 4(a). Each transition is labeled by spin states $|\xi_n^{N_1}\rangle$ of the ^1H spins.

The experimental protocol is described schematically in Fig. 4 (b). Starting from thermal equilibrium, we prepare $\rho_q^x(0)$ (see Eq. 15) using a $(\pi/2)_y$ pulse on ^{31}P followed by a CNOT gate U_c . Note that the CNOT gate is applied in parallel to all the ^1H spins exploiting the star-topology of the system. Then we use the CTP method to control the scrambling time t with fixed total time T as described in Fig. 1. The final state $\rho(t)$ is converted into the observable single quantum magnetization of the central spin using a second CNOT gate $U_c^\dagger = U_c$. The resulting signal is

$$\begin{aligned} s_q^x(t) &= \text{Tr} [(\sigma_x^P \otimes |\xi_n^{N_1}\rangle \langle \xi_n^{N_1}| \otimes \mathbb{1}^F) U_c^\dagger \rho(t) U_c] \\ &= \text{Tr} [U_c (\sigma_x^P \otimes |\xi_n^{N_1}\rangle \langle \xi_n^{N_1}| \otimes \mathbb{1}^F) U_c^\dagger \rho(t)] \\ &= \text{Tr} [U_c \{ |+\rangle^P \langle +|^P \otimes |\xi_n^{N_1}\rangle \langle \xi_n^{N_1}| \otimes \mathbb{1}^F \} U_c^\dagger \rho(t)] \\ &\quad - \text{Tr} [U_c \{ |-\rangle^P \langle -|^P \otimes |\xi_n^{N_1}\rangle \langle \xi_n^{N_1}| \otimes \mathbb{1}^F \} U_c^\dagger \rho(t)] \\ &= \text{Tr} [\rho_q^+(0) \rho(t)] - \text{Tr} [\rho_q^-(0) \rho(t)] \\ &= \text{Tr} [\rho_q^x(0) \rho(t)] \\ &= \mathcal{O}_q(t), \end{aligned} \quad (18)$$

where we have used Eq. 12 and 15. Thus OTOC can be directly extracted from the NMR signal $s_q^x(t)$ of the central ^{31}P spin.

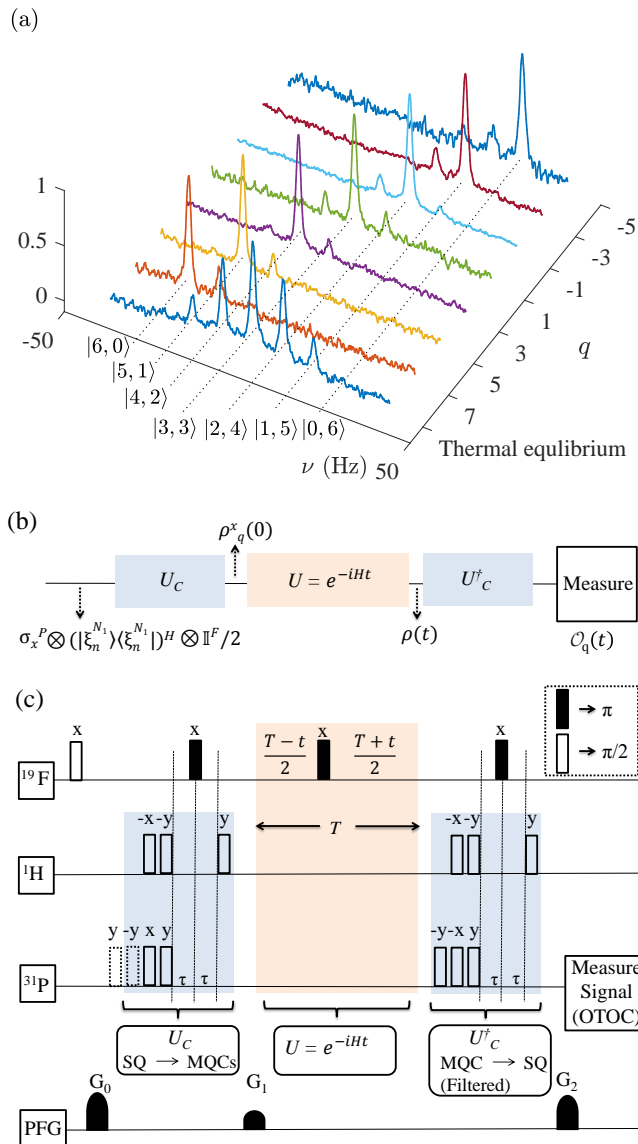


FIG. 4: (a) A reference ^{31}P NMR spectrum (first trace) and spectra corresponding to various quantum numbers q as indicated. The transitions are labeled by corresponding states $|\xi_n^{N_1}\rangle$ of ^1H spins. (b) Schematic illustration of the experimental protocol to study scrambling dynamics of MQCs. (c) The NMR pulse sequence to implement the protocol in (b). The open and filled rectangles correspond to $\pi/2$ and π rotation with phases as indicated. Here PFG denotes pulse field gradients along z -direction used to select a particular coherence pathway between MQCs and SQ (single quantum coherence) and $\tau = 1/4J$ indicates evolution time under coupling Hamiltonian given in Eq. 8.

The NMR pulse sequence for the preparation of the combination MQCs is shown in Fig. 4 (c). We start with the application of a $(\pi/2)_x$ pulse on ^{19}F spins followed by a pulsed-field-gradient (PFG) G_0 along z direction to prepare them in the maximally mixed $(\mathbb{1}/2)^{\otimes N_2}$ state. Subsequently a Hadamard gate using a $(\pi/2)_y$ is applied

on ^{31}P . The CNOT operation is realized via ^1H - ^{31}P J-coupling. During this period we refocus the interactions with ^{19}F spins using a $(\pi)_x$ pulse on ^{19}F . The unambiguous study of scrambling is carried out using the CTP method as described in the previous section (see Eq. 6). The time-reversal step in CTP is also realized using a $(\pi)_x$ pulse on ^{19}F . We vary the time parameter t by holding the total time T constant, so that the decoherence effects are same in all the experiments, while scrambling duration is systematically varied. Finally, MQCs are converted back to an observable single-quantum coherence. A specific MQC $\rho_q^x(0)$ of a particular quantum number q is filtered out by a pair of PFGs of strengths G_1 and G_2 as shown in Fig. 4 (c). The ratio of the PFGs to filter the q -quantum combination MQC is set to [27]

$$\frac{G_1}{G_2} = -\frac{\gamma_P + (q-1)\gamma_H}{\gamma_P}, \quad (19)$$

where γ_P and γ_H are gyro-magnetic ratios of ^{31}P and ^1H respectively.

Figs. 5 (a-c) display the experimentally measured OTOC functions corresponding to the quantum number $q = -1$ for various values of the nonintegrability parameter g . We have chosen $q = -1$ coherence because of its comparatively longer coherence time than the other MQCs. Fig. 5(a) displays OTOC evolution for $g = 0$ which belongs to the integrable regime and hence does not introduce scrambling. Here we are able to separate all three types of dynamics as follows:

- (i) Only decoherence (without unitary evolution $U(t)$): It is realized by effectively nullifying the interaction between ^1H spins of the first layer and ^{19}F spins of the second layer using a $(\pi)_x$ pulse on ^{19}F spins at the center of the time evolution. The decay profile leads to an effective coherence time $T_2^* \simeq 140$ ms (empty squares in Fig. 5(a)).
- (ii) Unitary dynamics along with decoherence: It is realized by allowing the interaction of ^1H spins with ^{19}F spins (triangles in Fig. 5(a)). This dynamics shows an oscillatory decay of OTOC, which in practical timescales of observation can be confused with the scrambling.
- (iii) Pure unitary dynamics - realized by CTP (circles in Fig. 5(a)). Here we observe almost decay-less oscillations with strong revivals of OTOC confirming the absence of genuine scrambling. The higher error bars, in this case, are due to lower signal to noise ratio.

Since case (ii) is the combined effect of the case (i) and (iii), one may expect the curve with triangles to match with the product of curves with squares and circles. However, here we find an interesting observation: the triangles over-shoot the empty squares at certain time instants (e.g. near $Jt = 1$) possibly signaling an information backflow due to non-Markovianity [30, 31].

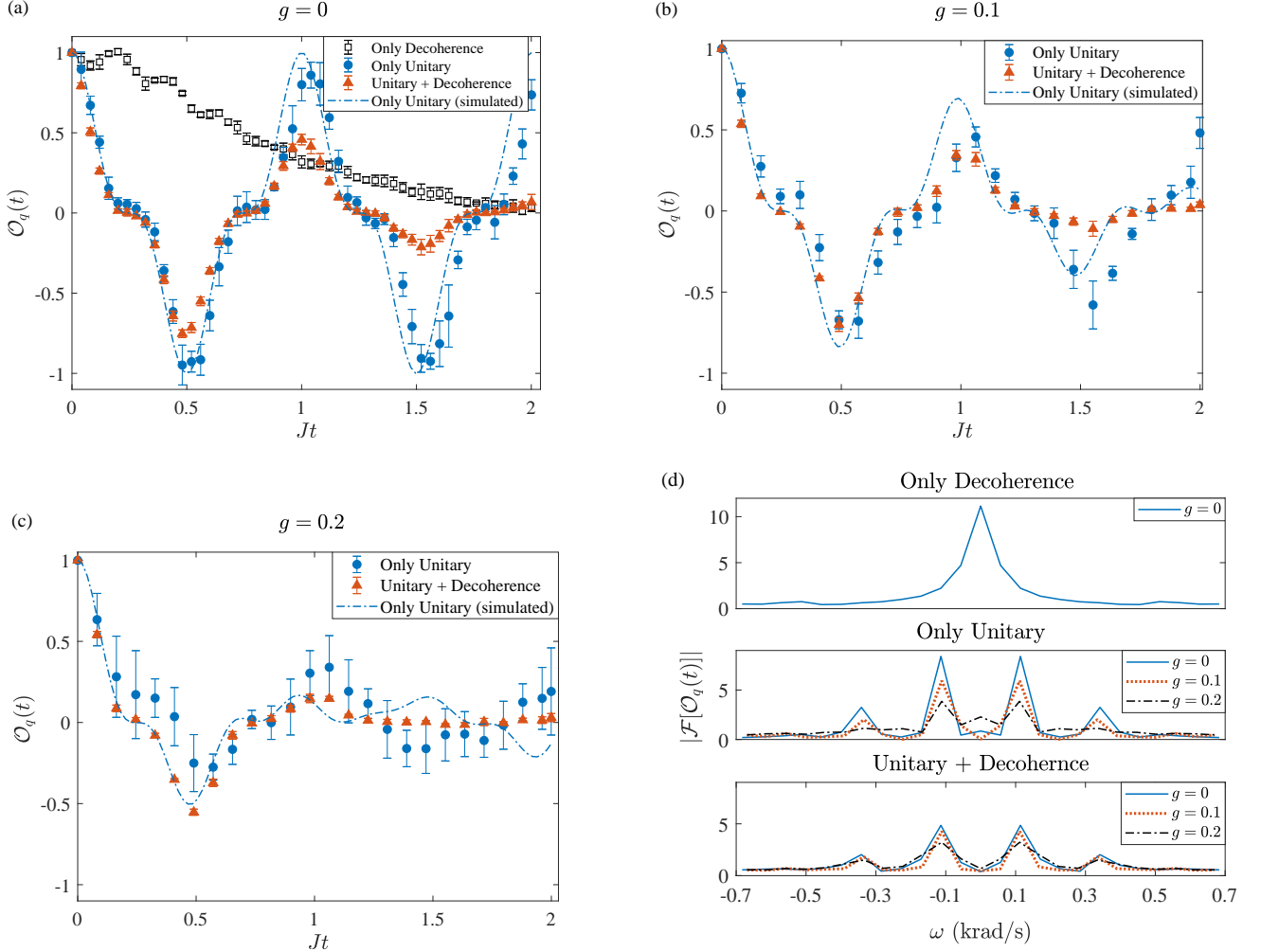


FIG. 5: Experimentally measured OTOC corresponding to time evolution of $q = -1$ quantum coherence in (a) integrable ($g = 0$) and (b-c) non-integrable ($g \neq 0$) regime. Dashed lines in (a-c) are obtained by numerical simulation using two-branch ($K = 2$) HSTS. Corresponding Fourier transform profiles are shown in (d).

In Fig. 5(b) and (c) we show time evolution of OTOC with $g = 0.1$ and $g = 0.2$ respectively. Here the presence of external fields leads to nonintegrable dynamics and consequently exhibit information scrambling. As a result, the OTOC does not show revivals back to the initial value. One can compare the OTOC data with unitary + decoherence in (a) (triangles) with OTOC data with only unitary (circles) in (c). While both show decaying revivals, the former is devoid of scrambling while the latter is purely due to scrambling. This suggests the importance of separating the decoherence effects before quantifying scrambling. Fig. 5(d) displays the Fourier transform of the OTOC data. As discussed in the previous subsection, we find broader and more dispersed spectral lines as we increase g , indicating stronger information scrambling.

V. CONCLUSIONS

In this work, we have studied scrambling of information in a double layered star-topology system. This topology allows us to efficiently prepare multiple quantum coherences involving central qubit and the first layer qubits. The scrambling is introduced in a controlled manner using the tunable external fields.

A major hurdle in the unambiguous study of scrambling is to account for the contribution from decoherence to OTOC dynamics. In this regard, we proposed a constant-time protocol which enables us to filter out contribution solely from scrambling.

Using a sixteen-spin double layered star-topology NMR system, we experimentally demonstrated the unambiguous study of scrambling of information stored in the combination multiple quantum coherence involving central qubit and six satellite qubits in the first layer. With the help of constant time protocol, we could clearly

separate decoherence effects and obtained OTOC profiles exclusively characterizing scrambling effects. While we observed signatures of non-Markovian evolutions, it calls for further detailed investigation in this direction.

Although the brute-force simulation of the complete system was computationally too expensive, it was nevertheless easier to tune the external field, control the scrambling rate and measure the OTOCs in the NMR spectrometer. In a way, it is a demonstration of the supremacy of quantum simulations over the classical analogs. Therefore, we expect to see more applications of such star-topology systems in studying many-body phenomena because of convenient manipulation allowed by higher symmetry.

Acknowledgments

This work was supported by DST/SJF/PSA-03/2012-13 and CSIR 03(1345)/16/EMR-II.

Appendix A: OTOC for highly mixed single-qubit initial state

Eq. 4 can be derived as follows

$$\begin{aligned} \mathcal{O}(t) &= \text{Re}[\langle B^\dagger(t)\rho^\dagger(0)B(t)\rho(0) \rangle_{\beta \rightarrow 0}] \\ &= \text{Re}[\text{Tr}\{B^\dagger(t)\rho^\dagger(0)B(t)(\rho(0))^2\}] \\ &= \text{Re} \left[\text{Tr} \left\{ B^\dagger(t) \left(\mathbb{1}/2 + \epsilon\rho_\Delta(0) \right) B(t) \left(\mathbb{1}/2 + \epsilon\rho_\Delta(0) \right)^2 \right\} \right] \end{aligned}$$

The right hand side produces following six terms

$$\begin{aligned} \frac{1}{8}\text{Re}[\text{Tr}\{B^\dagger(t)B(t)\}] &\rightarrow \frac{1}{4} \\ \frac{\epsilon}{2}\text{Re}[\text{Tr}\{B^\dagger(t)B(t)\rho_\Delta(0)\}] &\rightarrow 0 \\ \frac{\epsilon^2}{2}\text{Re}[\text{Tr}\{B^\dagger(t)B(t)(\rho_\Delta(0))^2\}] &\rightarrow \frac{\epsilon^2}{8}\text{Tr}\{(\rho_\Delta(0))^2\} \\ \frac{\epsilon}{4}\text{Re}[\text{Tr}\{B^\dagger(t)\rho_\Delta(0)B(t)\}] &\rightarrow 0 \\ \epsilon^2\text{Re}[\text{Tr}\{B^\dagger(t)\rho_\Delta(0)B(t)\rho_\Delta(0)\}] &\rightarrow * \\ \epsilon^3\text{Re}[\text{Tr}\{B^\dagger(t)\rho_\Delta(0)B(t)(\rho_\Delta(0))^2\}] &\rightarrow \text{negligible for } \epsilon \ll 1 \end{aligned}$$

As clear from the above, only the term indicated by * has information about the OTOC dynamics. Plugging these values back, we get

$$\begin{aligned} \mathcal{O}(t) &= \frac{1}{4} + \frac{\epsilon^2}{8}\text{Tr}\{(\rho_\Delta(0))^2\} \\ &\quad + \epsilon^2\text{Re}[\text{Tr}B^\dagger(t)\rho_\Delta(0)B(t)\rho_\Delta(0)], \end{aligned} \quad (\text{A1})$$

Hence

$$\mathcal{O}(t) \sim \text{Re}[\text{Tr}\{B^\dagger(t)\rho_\Delta(0)B(t)\rho_\Delta(0)\}], \quad (\text{A2})$$

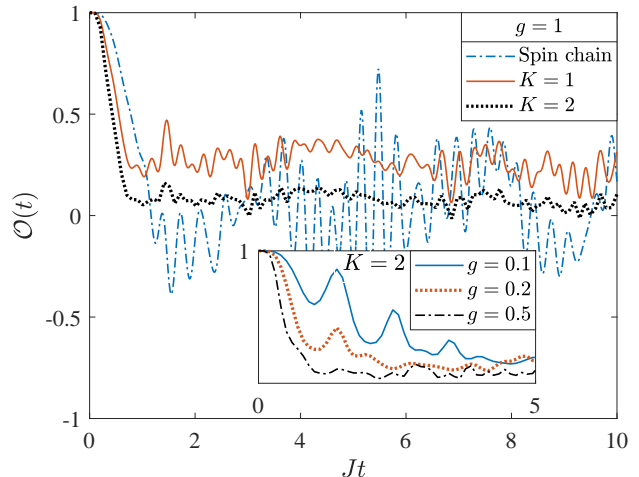


FIG. 6: Dynamics of OTOC for the experimental system shown in Fig 2. Here $A(0) = \sigma_y^P$ and $B(0) = S_y^F$ with $[A(0), B(0)] = 0$. The OTOC measures scrambling of information from the central qubit to the third layer. Though evolution in the presence of both x and z field is shown, Hamiltonian gives rise to scrambling even in the absence of z field. In the inset, variation of OTOC with the nonintegrability parameter g .

up to ϵ^2 factor and a constant background. It is interesting to note that, in NMR conditions, other measures of quantum correlations, such as Quantum Discord [32] and deviations in von Neumann entropy [33], are also measured in units of ϵ^2 .

Appendix B: Impact of system size and decoherence

It is useful to have some idea on how the extent of scrambling scales with the size of HSTS. In this regard, we consider the scrambling of information initially localized on the central spin (Fig. 2) onto the N_2 spins in the second layer via N_1 spins in the first layer. To this end, we choose

$$A(0) = \sigma_y^P \quad \text{and} \quad B(t) = U^\dagger(t)S_y^F U(t).$$

Since simulating the exact dynamics of the entire system with three branches consisting of 16 spins in Fig. 2 is computationally expensive, we limit ourselves to partial system sizes. For the integrable regime, i.e., nonintegrability parameter $g = 0$, OTOC function remains uniformly unity since the commutator $C(t)$ vanishes at all times owing to the fact that $B(t)$ can only develop multi-spin orders with protons in the first layer with which it is directly interacting. Hence information remains localized within the first layer and never scrambled onto the second layer. Even for small values of g , OTOC function deviates from unity and starts oscillating (see the inset of Fig. 6). Now we set $g = 1$ and look at the dependence

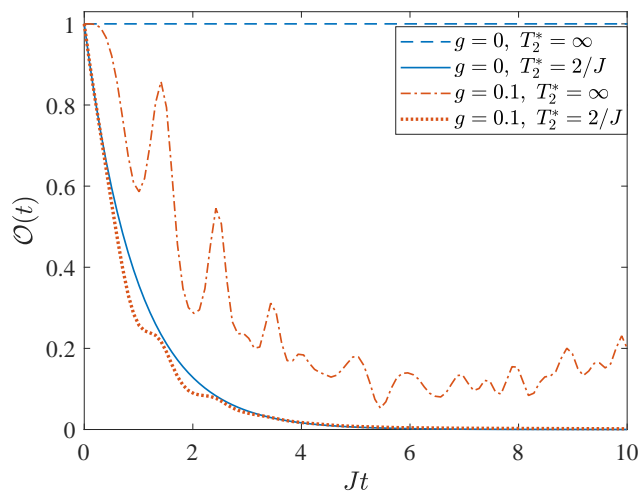


FIG. 7: Ambiguity in the estimation of information scrambling due to the presence of decoherence simulated using two-branch HSTS.

of scrambling on system size as shown in Fig. 6.

We use Lindblad based approach to simulate the combined effects of scrambling and decoherence with com-

pletely correlated dephasing model [24]. We introduce decoherence in the system by single-qubit dephasing modeled using the Lindblad equation

$$\frac{d\rho}{dt} = -i[H, \rho] + \gamma \sum_{i=1}^N (L_i \rho L_i^\dagger - \frac{1}{2} \{L_i^\dagger L_i, \rho\}), \quad (\text{B1})$$

where N is number of spins, $L_i = \sigma_z^i$ and $\gamma = 1/(2T_2^*)$ is transverse relaxation rate. To numerically simulate decoherence dynamics of OTOC, we update the density matrix in the following way

$$\rho(t) \rightarrow \gamma dt \sum_i L_i U(dt) \rho(t) U^\dagger(dt) L_i^\dagger + L_0 U(dt) \rho(t) U^\dagger(dt) L_0^\dagger, \quad (\text{B2})$$

where $L_0 = \sqrt{\mathcal{I} - \gamma dt \sum_i L_i L_i^\dagger}$ is no-jump operator. The above update can be interpreted as average over stochastic phase jump at each time step with probability γdt . As shown in Fig. 7, due to dephasing decay of OTOC in integrable regime almost overlaps with that of the non-integrable case for $T_2^* = 2/J$.

-
- [1] Stephen H Shenker and Douglas Stanford. Black holes and the butterfly effect. *Journal of High Energy Physics*, 2014(3):67, 2014.
- [2] Juan Maldacena, Stephen H Shenker, and Douglas Stanford. A bound on chaos. *Journal of High Energy Physics*, 2016(8):106, 2016.
- [3] Pavan Hosur, Xiao-Liang Qi, Daniel A Roberts, and Beni Yoshida. Chaos in quantum channels. *Journal of High Energy Physics*, 2016(2):4, 2016.
- [4] Martin Gärttner, Philipp Hauke, and Ana Maria Rey. Relating out-of-time-order correlations to entanglement via multiple-quantum coherences. *Physical review letters*, 120(4):040402, 2018.
- [5] Ken Xuan Wei, Chandrasekhar Ramanathan, and Paola Cappellaro. Exploring localization in nuclear spin chains. *Physical review letters*, 120(7):070501, 2018.
- [6] Yichen Huang, Yong-Liang Zhang, and Xie Chen. Out-of-time-ordered correlators in many-body localized systems. *Annalen der Physik*, 529(7):1600318, 2017.
- [7] Ruihua Fan, Pengfei Zhang, Huitao Shen, and Hui Zhai. Out-of-time-order correlation for many-body localization. *Science bulletin*, 62(10):707–711, 2017.
- [8] Yu Chen. Universal logarithmic scrambling in many body localization. *arXiv preprint arXiv:1608.02765*, 2016.
- [9] Markus Heyl, Frank Pollmann, and Balázs Dóra. Detecting equilibrium and dynamical quantum phase transitions in ising chains via out-of-time-ordered correlators. *Physical review letters*, 121(1):016801, 2018.
- [10] Sumilan Banerjee and Ehud Altman. Solvable model for a dynamical quantum phase transition from fast to slow scrambling. *Physical Review B*, 95(13):134302, 2017.
- [11] Ken Xuan Wei, Pai Peng, Oles Shtanko, Iman Marvian, Seth Lloyd, Chandrasekhar Ramanathan, and Paola Cappellaro. Emergent prethermalization signatures in out-of-time ordered correlations. *arXiv preprint arXiv:1812.04776*, 2018.
- [12] AI Larkin and Yu N Ovchinnikov. Quasiclassical method in the theory of superconductivity. *Sov Phys JETP*, 28(6):1200–1205, 1969.
- [13] Daniel A Roberts, Douglas Stanford, and Leonard Susskind. Localized shocks. *Journal of High Energy Physics*, 2015(3):51, 2015.
- [14] Brian Swingle, Gregory Bentsen, Monika Schleier-Smith, and Patrick Hayden. Measuring the scrambling of quantum information. *Physical Review A*, 94(4):040302, 2016.
- [15] Norman Y Yao, Fabian Grusdt, Brian Swingle, Mikhail D Lukin, Dan M Stamper-Kurn, Joel E Moore, and Eugene A Demler. Interferometric approach to probing fast scrambling. *arXiv preprint arXiv:1607.01801*, 2016.
- [16] Guangyu Zhu, Mohammad Hafezi, and Tarun Grover. Measurement of many-body chaos using a quantum clock. *Physical Review A*, 94(6):062329, 2016.
- [17] Nicole Yunger Halpern, Brian Swingle, and Justin Dressel. Quasiprobability behind the out-of-time-ordered correlator. *Physical Review A*, 97(4):042105, 2018.
- [18] Jun Li, Ruihua Fan, Hengyan Wang, Bingtian Ye, Bei Zeng, Hui Zhai, Xinhua Peng, and Jiangfeng Du. Measuring out-of-time-order correlators on a nuclear magnetic resonance quantum simulator. *Physical Review X*, 7(3):031011, 2017.
- [19] Mohamad Niknam, Lea F Santos, and David G Cory. Sensitivity of quantum information to environment perturbations measured with the out-of-time-order correlation function. *arXiv preprint arXiv:1808.04375*, 2018.

- [20] Kevin A Landsman, Caroline Figgatt, Thomas Schuster, Norbert M Linke, Beni Yoshida, Norm Y Yao, and Christopher Monroe. Verified quantum information scrambling. *Nature*, 567(7746):61, 2019.
- [21] Martin Gärttner, Justin G Bohnet, Arghavan Safavi-Naini, Michael L Wall, John J Bollinger, and Ana Maria Rey. Measuring out-of-time-order correlations and multiple quantum spectra in a trapped-ion quantum magnet. *Nature Physics*, 13(8):781, 2017.
- [22] Brian Swingle and Nicole Yunger Halpern. Resilience of scrambling measurements. *Physical Review A*, 97(6):062113, 2018.
- [23] Beni Yoshida and Norman Y Yao. Disentangling scrambling and decoherence via quantum teleportation. *Physical Review X*, 9(1):011006, 2019.
- [24] José Raúl González Alonso, Nicole Yunger Halpern, and Justin Dressel. Out-of-time-ordered-correlator quasiprobabilities robustly witness scrambling. *Physical review letters*, 122(4):040404, 2019.
- [25] Jonathan A Jones, Steven D Karlen, Joseph Fitzsimons, Arzhang Ardavan, Simon C Benjamin, G Andrew D Briggs, and John JL Morton. Magnetic field sensing beyond the standard quantum limit using 10-spin noon states. *Science*, 324(5931):1166–1168, 2009.
- [26] Deepak Khurana, Govind Unnikrishnan, and TS Mahesh. Spectral investigation of the noise influencing multiqubit states. *Physical Review A*, 94(6):062334, 2016.
- [27] Abhishek Shukla, Manvendra Sharma, and TS Mahesh. Noon states in star-topology spin-systems: Applications in diffusion studies and rf inhomogeneity mapping. *Chemical Physics Letters*, 592:227–231, 2014.
- [28] R Hanson, VV Dobrovitski, AE Feiguin, O Gywat, and DD Awschalom. Coherent dynamics of a single spin interacting with an adjustable spin bath. *Science*, 320(5874):352–355, 2008.
- [29] John Cavanagh, Wayne J Fairbrother, Arthur G Palmer III, and Nicholas J Skelton. *Protein NMR spectroscopy: principles and practice*. Elsevier, 1995.
- [30] Heinz-Peter Breuer, Elsi-Mari Laine, Jyrki Piilo, and Bassano Vacchini. Colloquium: Non-markovian dynamics in open quantum systems. *Reviews of Modern Physics*, 88(2):021002, 2016.
- [31] Inés De Vega and Daniel Alonso. Dynamics of non-markovian open quantum systems. *Reviews of Modern Physics*, 89(1):015001, 2017.
- [32] Hemant Katiyar, Soumya Singha Roy, TS Mahesh, and Apoorva Patel. Evolution of quantum discord and its stability in two-qubit nmr systems. *Physical Review A*, 86(1):012309, 2012.
- [33] VR Krithika, VS Anjusha, Udaysinh T Bhosale, and TS Mahesh. Nmr studies of quantum chaos in a two-qubit kicked top. *Physical Review E*, 99(3):032219, 2019.